Received: 16 November 2020 | Accepted: 19 February 2021 | Published online: 24 May 2021

DOI: 10.1002/saj2.20240

Soil Science Society of America Journal

SOIL PHYSICS & HYDROLOGY

Soil structure recovery following compaction: Short-term evolution of soil physical properties in a loamy soil

Thomas Keller[1,2] | **Tino Colombi**[2,3] | **Siul Ruiz**[4,5] | **Stanislaus J. Schymanski**[4,6] | **Peter Weisskopf**[1] | **John Koestel**[1,2] | **Marlies Sommer**[1] | **Viktor Stadelmann**[1] | **Daniel Breitenstein**[4] | **Norbert Kirchgessner**[3] | **Achim Walter**[3] | **Dani Or**[4,7]

[1] Agroscope, Dep. of Agroecology & Environment, Reckenholzstrasse 191, Zürich 8046, Switzerland

[2] Swedish Univ. of Agricultural Sciences, Dep. of Soil & Environment, Box 7014, Uppsala 75007, Sweden

[3] Swiss Federal Institute of Technology ETH, Institute of Agricultural Sciences, Universitätsstrasse 2, Zürich 8092, Switzerland

[4] Swiss Federal Institute of Technology ETH, Dep. of Environmental Systems Science, Universitätstrasse 16, Zürich 8092, Switzerland

[5] Univ. of Southampton, Dep. of Mechanical Engineering, Bioengineering Group, Southampton SO17 1BJ, UK

[6] Luxembourg Institute of Science and Technology, Environmental Research and Innovation Dep., Catchment and Eco-hydrology Research Group, 41 rue du Brill, Belvaux 4422, Luxembourg

[7] Desert Research Institute, Division of Hydrologic Sciences, 2215 Raggio Parkway, Reno, NV 89512, USA

Correspondence
Thomas Keller, Agroscope, Dep. of Agroecology & Environment, Reckenholzstrasse 191, Zürich, 8046 Switzerland
Email: thomas.keller@agroscope.admin.ch

Assigned to Associate Editor Vilim Filipović.

Funding information
Schweizerischer Nationalfonds zur Förderung der Wissenschaftlichen Forschung, Grant/Award Number: 406840-143061; National Research Fund, Grant/Award Number: ATTRACT programme (A16/SR/11254288)

Abstract

Soil compaction by farm machinery may persist for decades, hampering soil productivity and functioning. Assessing compaction costs and guiding recovery strategies are hindered by paucity of data on soil structure recovery rates. A long-term Soil Structure Observatory was established on a loamy soil in Switzerland to monitor soil structure recovery after prescribed compaction, and to better assess the roles of natural processes (vegetation, macrofauna, and shrink–swell cycles) on recovery patterns. The aim of this study was to quantify short-term soil structure recovery under natural conditions in the presence and absence of plant cover (ley and bare soil). We measured soil porosity and gas and water transport capabilities at 0.1 and 0.3 m depth. Two years after the compaction event, soil physical properties have not recovered to precompaction levels, even within the topsoil. Surprisingly, no differences were observed in the recovery patterns of ley and bare soil treatments. Measurements show that recovery rates differ among soil properties with the most severely affected properties by compaction (permeability) exhibiting highest recovery rates. Total soil porosity shows no recovery trend, suggesting lack of soil decompaction. Improved soil functions and decompaction are distinct aspects of soil structure recovery, with the latter requiring net upward transport of soil mass. We suggest that soil structure recovery proceeds at two fronts: from the soil surface downward, and expanding around local biologically-active pockets (marked by biopores) into the compacted soil volumes. This concept could be tested with additional data of longer time series at our site as well as in other soils and climates.

Abbreviations: SSO, Soil Structure Observatory.

1 | INTRODUCTION

Soil compaction of agricultural fields due to passage of tractors and implements is a major threat to soil productivity and its ecological and hydrological functioning. The persistent trend toward more powerful and heavier agricultural vehicles is aggravating this acute but often poorly diagnosed threat of soil compaction (Keller et al., 2019). Despite challenges to reliably quantify the direct damage of soil compaction, estimated costs in terms of loss of soil functioning and reduced productivity are substantial (Graves et al., 2015; Sonderegger et al., 2020). Evidence suggests that compaction affects 25–45% of arable land area of modern mechanized agriculture in Europe (Brus & van den Akker, 2018; Schjønning et al., 2015). The associated costs of soil compaction vary with soil type, climate, and levels of mechanization. Compaction is not restricted to arable lands only with compaction signatures found under different soil management and land use, such as use of construction machinery (Berli et al., 2004) or military maneuvers (Vennik et al., 2019). The management of permanent grassland often involves the use of heavy equipment (harvest, manure and slurry spreading) with associated risks of soil compaction (Bouwman & Arts, 2000). Pastures may also be compacted by grazing animals (Greenwood & McKenzie, 2001). In addition to agricultural soils, forest soils may be compacted during logging and harvest operations (DeArmond et al., 2019; Nordfjell et al., 2019), and soils in natural ecosystems may be at risk of compaction by grazing animals, hikers, and any type of off-road vehicle traffic (Kissling et al., 2009; Waever & Dale, 1978).

The economic and ecological consequences of compaction result from a complex function of the magnitude of the compaction event (i.e., the immediate change of soil functions following the compaction event) and the recovery time to precompaction conditions (Keller et al., 2017). In other words, compaction costs are incurred over the cumulative loss of soil functions integrated over the recovery time. The effects of compaction are relatively well documented (Håkansson et al., 1988; Horn et al., 1995; Lipiec & Hatano, 2003; Nawaz et al., 2013); however, much less information is available on the rates of soil function and structure restoration from compaction. Evidence from field studies suggests that recovery of compacted soil, especially subsoil, is an exceedingly slow process extending over periods of decades or even centuries (Schjønning et al., 2015).

Whereas compacted soil surfaces may be rapidly loosened by soil tillage, tillage does not simply "uncompact" a compaction-damaged soil. Tillage may increase soil bulk porosity and reduce mechanical impedance in the tilled layer; however, tillage-created soil fragments remain largely compacted and lack ecological traits of uncompacted soil. Consequently, compaction effects often persist in the topsoil for several years even under conventional tillage (Arvidsson & Håkansson, 1996; Weisskopf et al., 2010). Tillage is mostly restricted to the upper 0.1–0.3 m depth of the soil profile. Occasional subsoiling may loosen deeper layers, but this is not a sustainable soil management option. In addition, subsoiling may often not result in the expected positive effects (Olesen & Munkholm, 2007). This implies heavy reliance of arable subsoils and untilled soils such as no-till, rangelands, and forests soils on natural soil structure recovery processes.

Core Ideas

- Soil physical properties have not recovered to precompaction values within 2 yr.
- Recovery rates vary among soil physical properties.
- Decompaction (increase in total porosity) requires upward transport of soil mass.
- Functional recovery such as improved permeability does not require decompaction.
- A concept for soil structure recovery patterns is proposed.

Key processes of natural recovery of compacted soil have been extensively studied. These include abiotic processes (soil shrinkage and swelling induced by drying and wetting or freezing and thawing), biotic processes (root penetration, burrowing by earthworms and other soil fauna, changes in surface properties due to microbial activity), and combined biotic–abiotic processes (shrinkage of soil induced by root water uptake, soil aggregation) (Dexter, 1991). What is lacking for prediction of soil structure and function restoration is a quantitative description of rates and ranking of the relative importance, interactions, and feedbacks among these key processes. Because compaction results in a decrease in soil total porosity, decompaction must involve an increase in overall porosity. However, a change in overall porosity is not a prerequisite for the restoration of certain ecological and hydrologic functions. One such example is root penetration, which may result in new continuous macropores that, after roots have decayed, improve soil aeration and infiltration without any change in total porosity (Dexter, 1987a). On the other hand, certain recovery processes such as tillage may decompact the soil (i.e., increases in pore volume) without greatly improving other functions such as gas exchange (Weisskopf et al., 2010). Knowledge of compaction recovery is based on a few field studies that measured a limited number of soil properties at different times after a compaction event (e.g., Berisso et al., 2012; Blackwell et al., 1985; Peng & Horn, 2008) or land use change (Beck-Broichsitter et al., 2020), often with poor temporal resolution (e.g., only two sampling times, shortly after compaction and several years later). Besson et al. (2013) reported

limited soil structure recovery after compaction in a silt loam soil but their study was limited to 1 yr of observations. Gregory et al. (2007) monitored penetration resistance in three soils during 1.3 yr following compaction and concluded that coarse textured soils are less resilient to compaction stress. Laboratory and lysimeter studies have contributed some quantitative information on compaction recovery, but typically addressed one or two processes only (drying–wetting, Barzegar et al., 1995; freezing–thawing, Viklander, 1998; drying–wetting and freezing–thawing, Arthur et al., 2012; Gregory et al., 2009; root penetration, Pulido-Moncada et al., 2020). Arthur et al. (2013) performed experiments with sieved soil in boxes placed outdoors and reported that clay type was a crucial factor for soil structure evolution. There is a need for a more mechanistic description of how compacted soil recovers that captures time scales of respective processes and disentangles these processes with respect to their contribution to functional recovery and decompaction.

To obtain systematic information necessary for quantifying soil structure recovery rates following compaction, we initiated a long-term field experiment, termed the Soil Structure Observatory (SSO). The primary objectives of the SSO were to monitor soil structure recovery after compaction considering different compaction patterns and postcompaction soil management treatments. The experiment, arranged in three replicates, permits the quantification of soil structure and function recovery rates under natural conditions with and without plants and under crop rotations with and without tillage (Keller et al., 2017). The aim of this study was to quantify short-term soil structure recovery under natural conditions in the presence and absence of plant cover (ley and bare soil) during the first 2 yr after compaction. We measured soil macropore features and soil gas and water transport properties, and discussed mechanisms of soil structure recovery. This study addresses the following research questions:

- Are the temporal characteristics of recovery different for different soil physical properties?
- How does recovery of physical properties vary with soil depth?
- How does the presence or absence of vegetation affect soil structure recovery?

We hypothesized that recovery rates (a) differ between soil physical properties, (b) are not constant over time, and (c) are promoted by vegetation (and associated biological activity).

2 | MATERIALS AND METHODS

2.1 | Experimental site and design

The study summarizes observations obtained from the SSO, located near Zürich, Switzerland (47.4° N and 8.5° E, 444 m asl). The SSO has two experimental factors (compaction level and postcompaction soil management, see below) in a strip-plot design with three field replications of each compaction by management combination (plot size is 10 m by 17 m; total experimental area ∼1 ha). A detailed description of the SSO is reported in Keller et al. (2017). The soil is a deep gleyic Cambisol (IUSS Working Group WRB, 2015) with a loamy texture (average texture 27% clay, 48% silt, 25% sand). Soil organic C content is 1.7% in the topsoil (0–0.2 m depth), 0.8% in the subsoil (0.3–0.5 m depth), and average soil pH($CaCl_2$) is 6.9. A meteorological station from the Swiss Federal Office of Meteorology and Climatology (MeteoSwiss) is located within 200 m of the experimental site. Mean annual temperature is 9.4 °C, and mean annual precipitation is 1,054 mm.

In preparation for the compaction experiment, the site was sown (April 2013) with a perennial grass–legume mixture (SM 442; Suter et al., 2008) reinforced with an additional 4 kg ha^{-1} of lucerne (*Medicago sativa* L.). Prior to the establishment of our experiment, the experimental site was a conventionally managed arable field (arable crop rotation, conventional soil, and crop management with moldboard plowing to about 0.25 m depth). The primary treatment for the SSO was a one-time compaction event in March 2014, using three passes of a self-propelled two-axle agricultural vehicle (front wheel load 8,900 kg, rear wheel load 7,200 kg; 1,050/50R32 tires on all wheels with an inflation pressure of 330 kPa). We focus here on monitoring physical soil properties from two compaction levels: compaction of the entire plot area (track-by-track; Figure 1a), and control (i.e., no experimental compaction). Following the compaction under moist conditions (soil matric potential slightly decreasing between −60 hPa at 0.1 m depth to −100 hPa at 0.7 m depth; Keller et al., 2017) in March 2014, four postcompaction soil management treatments were established: permanent ley (continuation of the in-sown lay), bare soil, crop rotation without tillage, and crop rotation with tillage. In this study we present data from the ley and bare soil treatments. The SSO is arranged as a block design with three replications (Keller et al., 2017). Because the compaction treatment was applied on the ley that was sown uniformly over the entire experimental site 1 yr prior to compaction, all postcompaction management treatments (ley, bare soil) started with similar conditions. For the bare soil treatment, we terminated the ley immediately after compaction using herbicides.

Following the compaction treatment, no machinery traffic or other soil disturbances (tillage) were permitted in the ley and the bare soil treatments apart from a one-axle motor mower (total mass ∼200 kg) to cut the ley. Hence, we consider observations from these treatments as indicative of natural soil structure recovery in the presence and absence of plants, respectively. For the bare plots, we suppressed emergence and establishment of vegetation through periodic application of nonselective herbicides (frequency, dosage, and

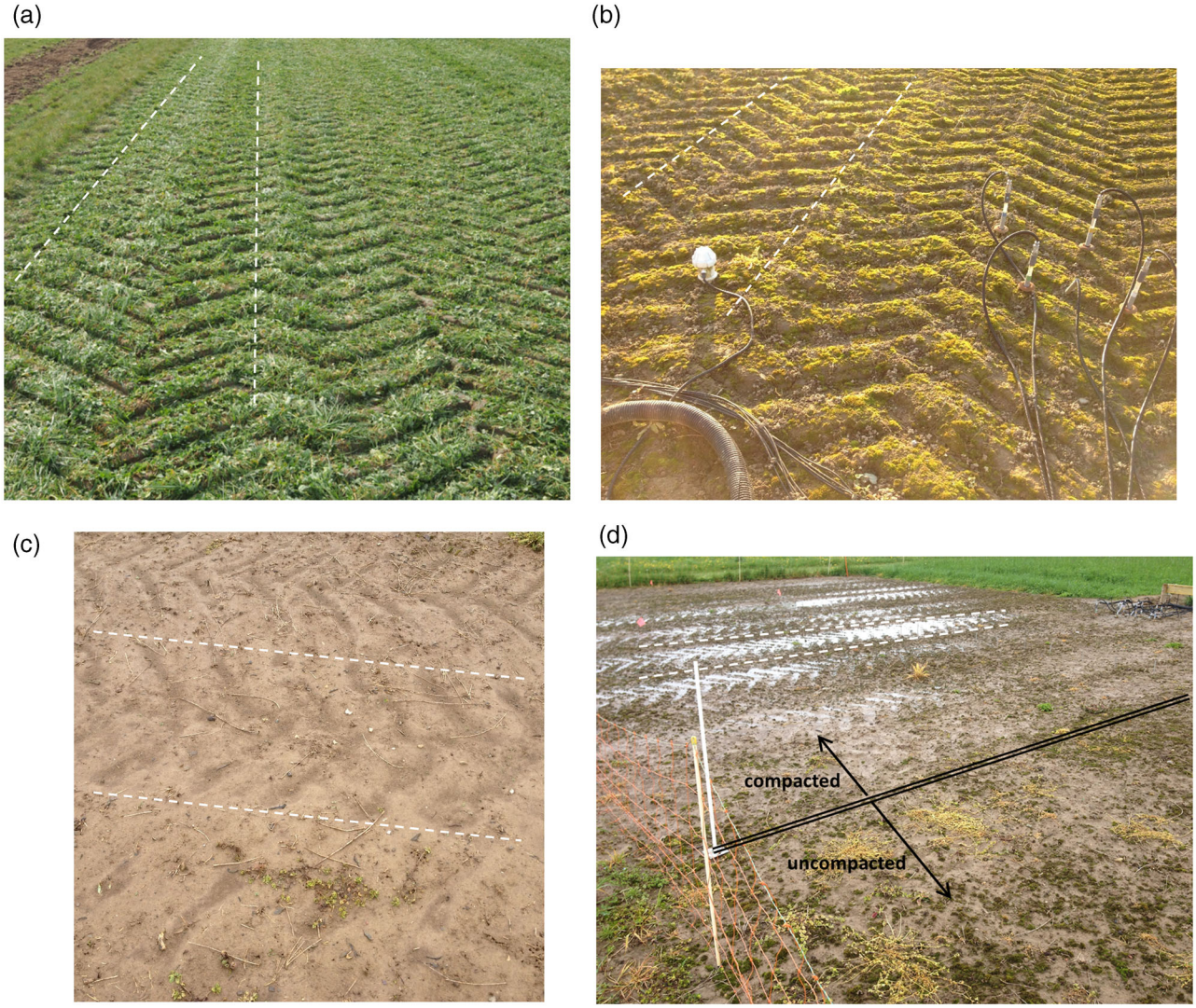

FIGURE 1 Impressions from the experimental site. Soil surface of the track-by-track treatment (compaction of the entire plot area; tire width 1.05 m, one tire track is indicated by dashed white lines in each photo) (a) at the day of compaction infliction (end of March 2014) after the passage of the two-axle self-propelled agricultural vehicle, (b) at the end of October 2014 (7 mo after compaction), and (c) in the beginning of May 2015 (13 mo after compaction). (d) Ponding water in the compacted plot of the bare soil treatment in the beginning of May 2016, 25 mo after the compaction event

herbicide product based on need). Occasional growth of weeds cannot be avoided but was kept at a minimum as herbicide application was frequent. The ley was cut 4–5 times per year and manually removed from the experimental plots.

Sampling and measurements of all soil properties described in this study were made in autumn 2013 (approximately 5 mo before compaction), in spring 2014 shortly after compaction, and about 6 mo (autumn 2014), 12 mo (spring 2015), and 24 mo (spring 2016) after compaction. That is, the sampling frequency was higher (every 6 mo) during the initial phase of the experiment. All in situ measurements and sampling were done at similar soil moisture conditions (around field capacity). Characterization of the precompaction state (autumn 2013) involved sampling and measurements at 12 randomly selected locations in each experimental block. Coefficients of variations within each block and depth for precompaction measurements (Keller et al., 2017) were 3–5% for total porosity and 20–28% for saturated hydraulic conductivity. All post-compaction measurements were done at the plot level at 2–3 randomly selected locations in each experimental plot.

2.2 | Water infiltration

We measured steady-state infiltration at the soil surface at three locations per experimental plot using a constant head single-ring infiltrometer (diameter 0.2 m) (Perroux & White, 1988). After placing the ring, vegetation inside the ring was cut with scissors as close to the soil surface as possible without disturbing the soil, worm casts were collected, and stones

or lumps of soil that extended above the rim of the ring were carefully removed. No material was added to level the ground. If the ground inside the randomly placed ring was too uneven for the measurement, a new random location was chosen. The applied pressure head was about 5 mm (Perroux & White, 1988) and the rate of infiltration was deduced from the drop in water reservoir with time and translated to a cumulative infiltration vs. time relationship.

2.3 | Soil penetration resistance

Soil penetration resistance was measured with five random insertions per plot to 0.8 m depth using an Eijkelkamp penetrologger with a cone base of 1 cm^2 and a cone angle of 60° (Eijkelkamp Soil & Water). For further analysis in this study, we calculated the average penetration resistance at 0.05–0.15 m (mean 0.1 m depth) and 0.25–035 m (mean 0.3 m depth) for each plot and sampling date. Due to a malfunction of the penetrometer device, data from autumn 2013 and spring 2014 had to be discarded.

2.4 | Soil core sampling and measurements

Undisturbed cylindrical soil cores (diameter 0.05 m, height 0.05 m) were sampled at the 0.1 and 0.3 m depth (depths refer to the center of a soil core) using an Eijkelkamp sample ring kit model C (Eijkelkamp Soil & Water). We used custom-made sample rings in aluminum that are better suited for use in an x-ray scanner (Section 2.4). At each sampling event, we collected three (spring 2014) or two (autumn 2014, spring 2015, spring 2016) soil cores per plot and depth. The difference in number of sampling points reflects characterization of the compaction impact (spring 2014) and monitoring (autumn 2014 and subsequent sampling events). Moreover, we compromised on the number of samples per plot and depth in favor of being able to sample more frequently. The samples were stored at 2 °C until further processing. A similar measurement procedure was applied to all samples. The soil samples were gradually saturated from below and then drained to a matric potential of −10 kPa on ceramic plates (Ecotec). Next, we measured air permeability and then gas diffusivity. Air permeability was obtained by measuring the air flow through the sample at an overpressure of 2 hPa, and gas diffusivity was measured in a one-chamber apparatus that uses O_2 as the diffusing gas assuming steady-state diffusion; both methods are described in Martínez et al. (2016). Next, we randomly selected one sample per plot and depth and scanned them using three-dimensional x-ray computed tomography for quantification of soil macropore architecture as detailed below. For this, samples were drained to −30 kPa to ensure all visible pores were air-filled. All samples were saturated again and saturated hydraulic conductivity was measured using the constant head method (Klute & Dirksen, 1986). Hereby, the pressure was adjusted for each sample to ensure laminar flow (average pressure ∼5 kPa). Finally, all samples were dried in an oven at 105 °C for at least 24 h and then their dry weight was determined, which served as a basis for the calculation of bulk density, soil water contents, and air-filled porosities at each matric potential.

2.5 | X-ray micro-computed tomography: Image acquisition, processing, and analysis

All x-ray images were acquired using a GE Phoenix v|tome|x 240 S industrial x-ray scanner with a four megapixel detector (GE DRX250). Scanner setup and reconstruction parameters are given in Supplemental Table S1. We deliberately compromised on the resolution (and hence the detectable features) using binning in favor of being able to scan more samples. The obtained image voxel size of 60 µm allows for detection of objects with diameters of approximately 120 µm or larger.

We used ImageJ/Fiji (Schindelin et al., 2012; Schneider et al., 2012) with the SoilJ plugin (Koestel, 2018) to process and evaluate the three dimensional x-ray images (parameters are summarized in Supplemental Table S1). Soil column outlines within each image were automatically detected using SoilJ. We applied a median filter with a radius of two voxels to reduce image noise, followed by an unsharp mask with SD of two voxels and a weighting factor of 0.6 to sharpen phase boundaries in the images. We compensated for residual beam-hardening, using an exponential function to capture averaged radial brightness biases. The greyscale of all three-dimensional images was calibrated to the grey-value of the column wall (aluminum) and the 0.1 percentile of the grey-values corresponding to soil (the latter serves as a proxy for the grey-value of air filled pores; Koestel et al., 2018). The greyscale calibration process was applied on individual horizontal image layers, which enables the correction of image illumination biases in the vertical direction (Koestel, 2018). We then calculated two-dimensional histograms (featuring the grey-values and their first spatial derivative) of all three-dimensional x-ray images and segmented the x-ray images into three distinct image phases (air-filled macropores, particulate organic matter including roots, and all denser imaged phases) as described in Koestel and Schlüter (2019).

We used SoilJ in combination with two other ImageJ plugins, MorphoLibJ (Legland et al., 2016) and BoneJ (Doube et al., 2010), to quantify the morphology of the imaged air-filled macropore network. We investigated the macroporosity (m^3 m^{-3}), the macropore surface area (m^2), the critical pore diameter (m) and the hydraulic radius (m), as well as three connectivity measures: the connection probability, also known as Γ-connectivity (-), the Euler-Poincaré number (-),

and the percolating porosity ($m^3\ m^{-3}$). We refer to Jarvis et al. (2017) for a detailed description of these properties.

2.6 | Earthworm biomass and surface cast production

Earthworms were collected in a squared area of 0.25 m^2, with two replicates in each experimental plot. First, we excavated the top 0.3 m and collected earthworms by hand sorting. Then, a 0.5% formaldehyde solution was applied to extract earthworms from the subsoil (Kramer et al., 2008). Adults were determined to the species level and juveniles to ecological groups. An estimate of earthworm egestion rates at the soil surface was obtained in 2014 by collecting earthworm casts on the surface. Two locations were randomly selected in each plot, and casts were collected within circular areas of 0.2 m diameter at each location.

2.7 | Soil state variables monitored in the SSO

The SSO includes an extensive network of soil-embedded sensors used for continuous in situ measurements of state variables (soil water content, soil matric potential, soil temperature, O_2 diffusion rate, redox potential, and O_2 and CO_2 concentrations) at various depths (see Keller et al. [2017] for details). The sensors were installed in two of the three experimental blocks. In this study, we present data on soil water contents and on O_2 concentrations in soil air. Water contents were measured using in-house–produced two-prong (~0.15 m length) time-domain reflectometry probes (Jones et al., 2002), with two probes per plot and depth and recorded every 30 min. Soil O_2 concentrations were measured biweekly from porous polypropylene tubes inserted in the soil at various depths (two tubes per plot and depth) using a CheckMate 9900 head space analyzer (PBI Dan-sensor A/S) as described in Weisskopf et al. (2010).

2.8 | Statistical analyses

Data were analyzed with linear mixed models followed by analysis of covariance using the nlme package in R (Pinheiro et al., 2021). The effects of compaction, postcompaction management (ley, bare soil), and their interaction were set as fixed factors, and the sampling time point was set as a fixed covariable. To account for repeated measurements, the plot effect was set as a random factor. Results obtained at different depths were analyzed separately. The statistical model is given in Supplemental Figure S1, Equation S1. In addition, treatment mean values within one sampling time were compared using LSD tests at $p < .05$ as implemented in the R-package agricolae (de Mendiburu, 2017). Furthermore, we calculated Pearson correlation coefficients between properties obtained from x-ray imaging (Section 2.4) and fluid transport properties (air permeability, gas diffusivity, saturated hydraulic conductivity).

3 | RESULTS

Images from the experimental site at various points in time after compaction are shown in Figure 1 for general impression of compaction effects. The soil surface on the day of compaction after the passage of the vehicle is depicted in Figure 1a. The tire imprints (tire lug pattern) were clearly visible 7 mo (Figure 1b) after compaction, and still recognizable 1 yr (Figure 1c) and 2 yr (Figure 1d) after compaction. The first winter with occasional snow cover led to slaking and surface levelling in the bare soil plots (Figure 1c). Compaction effects on water infiltration capacity are obvious after rain events as shown in Figure 1d.

3.1 | Infiltration at the soil surface

Following compaction, the rate of surface water infiltration significantly decreased ($p < .05$) by three orders of magnitude from ~10 mm min^{-1} to ~0.01 mm min^{-1} (Figure 2). We observed a rapid recovery of infiltration rates 6 mo after compaction, the infiltration rates were about 1 mm min^{-1} in the compacted plots irrespective of vegetation cover (Figure 2). Soil recovery continued in the ley treatment during winter, and 1 yr after compaction (spring 2015) there was no significant difference ($p > .05$) in infiltration between compacted and control plots of the ley treatment (Figure 2). It is unlikely that the very brief freezing and thawing events had significantly contributed to improved infiltration, as air temperature was only occasionally below zero in Zürich (on average 21 d per year with mean air temperature below 0 °C; Supplemental Figure S1). For the bare soil, the improvement in infiltration during winter 2014–2015 was marginal (Figure 2), and infiltration in bare soil was significantly lower ($p < .05$) than in the ley treatment in spring 2015. Apart from a tendency of decreasing infiltration in the compacted bare soil treatment, no changes in infiltration were measured between 1 yr (spring 2015) and 2 yr (spring 2016) after compaction (Figure 2).

3.2 | Soil penetration resistance, bulk density, porosity, and fluid transport properties

As expected, the soil bulk density increased significantly (and total porosity decreased) due to compaction at the measured

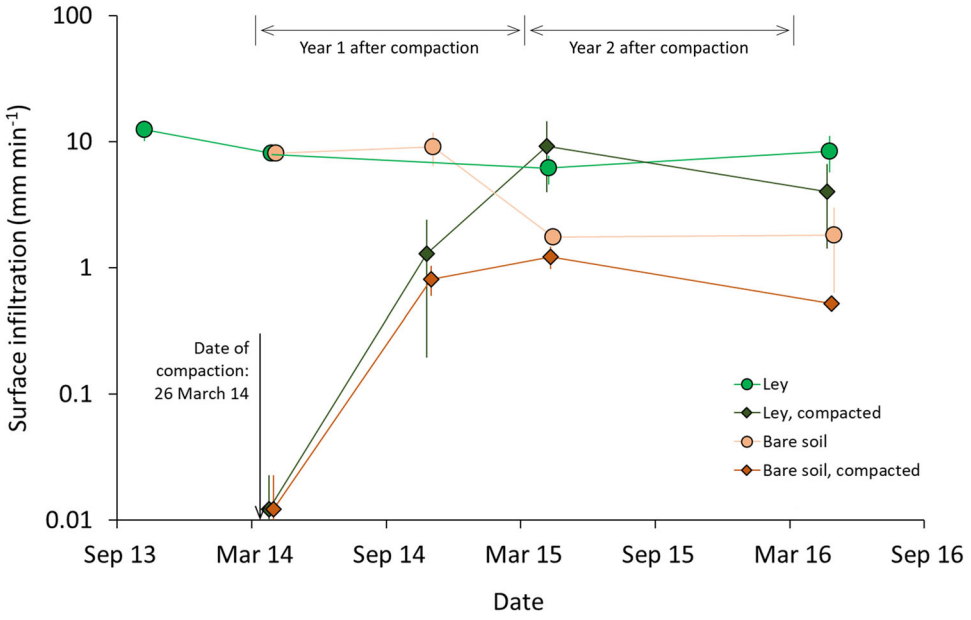

FIGURE 2 Infiltration at the soil surface of the compacted and noncompacted (control) plots of the ley and bare soil treatments. Error bars represent SE ($n = 3$)

0.1 and 0.3 m depths ($p < .05$; Supplemental Table S2). Compaction significantly increased penetration resistance and reduced air-filled porosity, gas diffusivity, air permeability, and saturated hydraulic conductivity ($p < .05$; Supplemental Table S2 and S4), with effects more pronounced at 0.1 than at the 0.3 m depth. Compaction affected various soil physical properties to different extents, with the smallest relative reduction (~5% at 0.3 m depth and ~15% at 0.1 m depth) for bulk density (Figure 3) and the largest reduction (one to two orders of magnitude) for air permeability (Figure 4).

The temporal evolution of soil physical properties at 0.1 and 0.3 m depths for the ley and bare soil treatments within the first 2 yr after compaction are shown in Figures 3 and 4 and Supplemental Figures S2–S5. We did not find any significant change with time for any of the measured properties obtained from soil core samples (i.e., no significant recovery trends [$p > .05$; Supplemental Table S2]). Soil penetration resistance revealed significant changes with time (Supplemental Table S4), but these were not associated with recovery (Supplemental Figure S5). Bulk density and penetration resistance showed no signs of recovery (Figure 3; Supplemental Figure S5). Trends of recovery were observed for air permeability (Figure 4), air-filled porosity, gas diffusivity, and saturated hydraulic conductivity (Supplemental Figures S2–S4). When comparing treatments for each sampling time separately, differences between compacted and noncompacted plots were generally still significant ($p < .05$) 2 yr after compaction for penetration resistance, bulk density, and air-filled and total porosity, whereas they were not statistically significant anymore ($p > .05$) for gas diffusivity, air permeability, and saturated hydraulic conductivity (Supplemental Tables S5 and S7). Nonsignificant difference for the latter may also be related to the generally higher variability of fluid transport properties than bulk properties in combination with the limited number of field replicates (three experimental blocks; Section 2.1). Considering the fact that all measured values were consistently lower (porosity, fluid transport properties) and consistently higher (bulk density, penetration resistance), respectively, in the compacted than in the noncompacted soil, the statistical analyses indicate very limited recovery for bulk properties (porosity, bulk density, penetration resistance) and trends of recovery for functional soil properties (gas and water transport) within the first 2 yr after compaction.

From soil bulk density measurements, we recognize a certain degree of temporal variability between sampling times (Figure 3), which could be due to swell–shrink effects (as soil moisture conditions were slightly variable between sampling times; e.g., Goutal et al., 2012) and spatial variability within experimental plots. To better reveal trends related to compaction recovery, and minimize impacts due to temporal variability between samplings of soil properties of control plots, we plotted relative values as the ratio of measured data on compacted plots to measured data on noncompacted plots for each sampling time. This made differences in impact of compaction and differences in recovery rates among soil properties evident (Figure 5). Generally, properties that were most severely affected by compaction showed signs of recovery. Total porosity revealed no signs of recovery, whereas an increase in air-filled porosity, gas diffusivity, and air permeability was measured during the first year following compaction (Figure 5). However, measurements revealed little

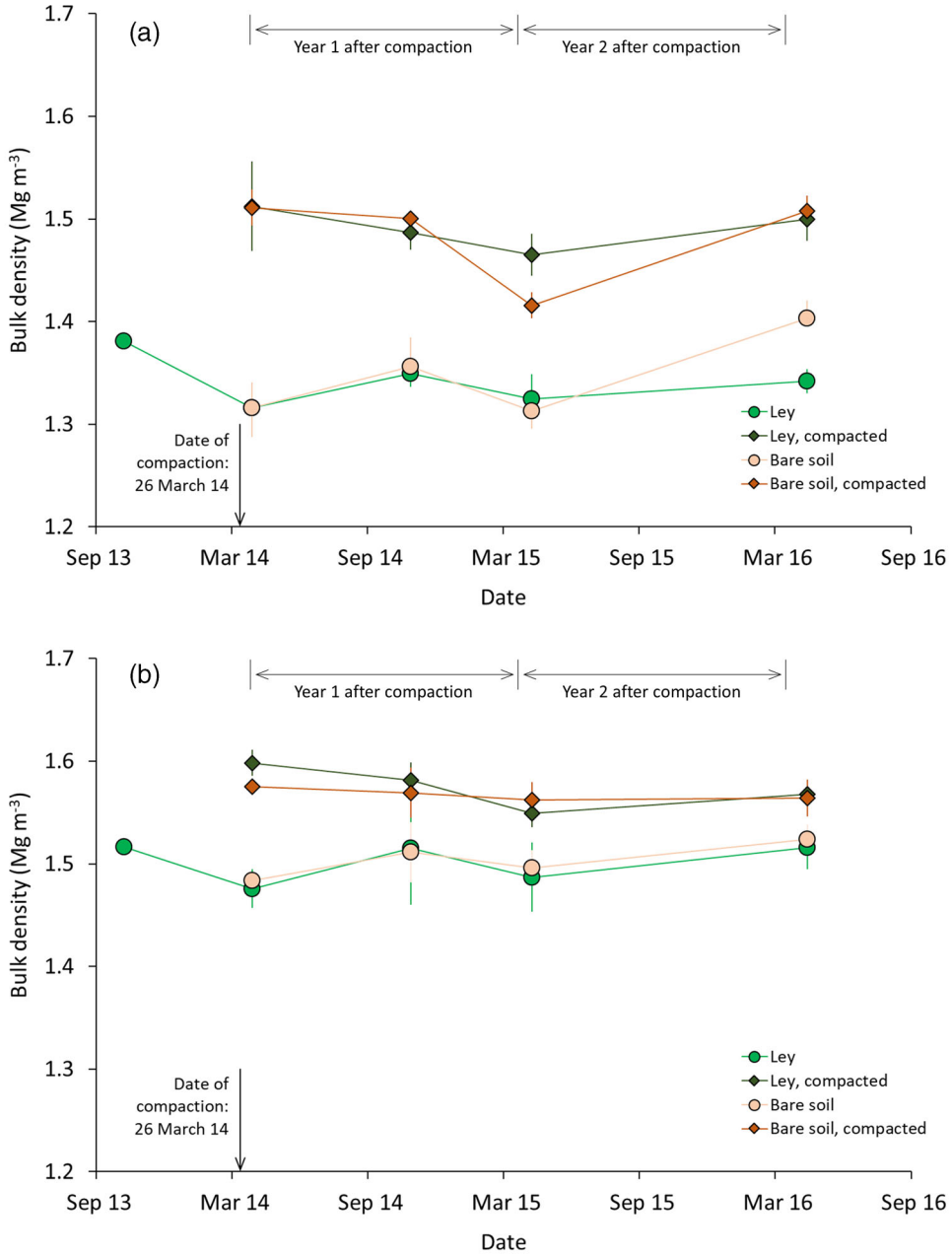

FIGURE 3 Evolution of bulk density at (a) 0.1 m and (b) 0.3 m depth as a function of time after compaction. Error bars represent SE ($n = 3$)

signs of recovery during the second year following compaction for any soil property (Figure 5). The constancy of soil bulk density or total porosity in the compacted treatments (Figures 3 and 5) indicates that decompaction by upward transport of soil particles and internal soil volume expansion were limited.

Little differences between the ley and the bare soil treatment (Figures 3 and 4; Supplemental Figures S2–S4) suggest that the presence or absence of vegetation had no significant effect ($p > .05$; Supplemental Table S2) on the recovery of soil physical properties in the first 2 yr following compaction. However, we observed a tendency toward deteriorating physical properties in the bare soil treatments during the second year following compaction (Figure 4; Supplemental Figures S2–S4).

3.3 | Macropore system architecture based on computed tomography imaging

Figure 6a shows illustrative examples of cross-sections through soil core samples before compaction, immediately after compaction, and 2 yr after compaction. The differences in porosity are clearly visible with numerous macropores (rounded pores are presumably biopores and planar pores are presumably shrinkage cracks) present before compaction,

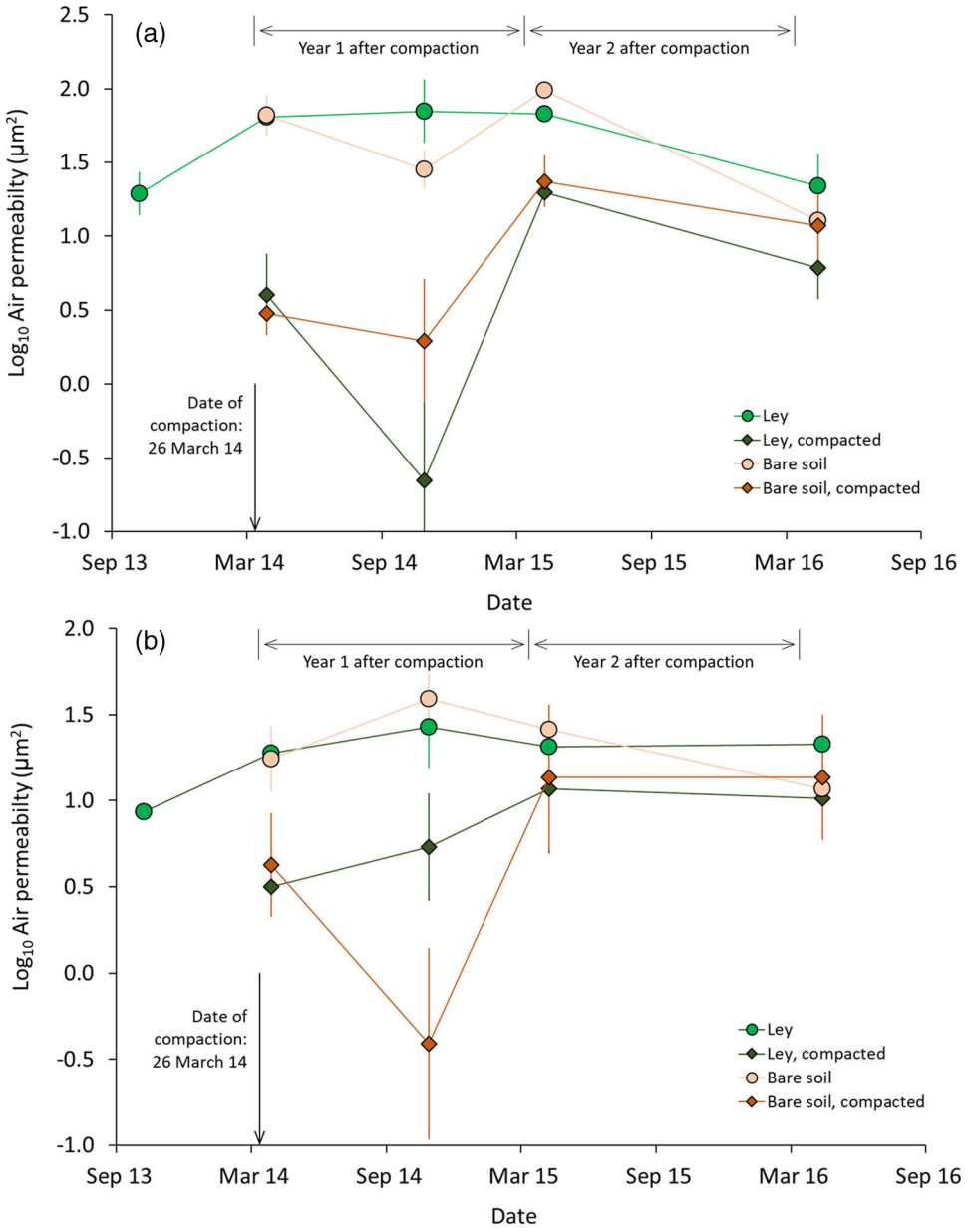

FIGURE 4 Evolution of air permeability at a matric potential of −10 kPa at (a) 0.1 m and (b) 0.3 m depth as a function of time after compaction. Error bars represent SE ($n = 3$)

only a few remaining macropores after compaction, and a gradual reappearance of macropores 2 yr after compaction. Deduced macroporosity (equivalent pore diameter >120 µm) decreased due to compaction by more than 80% (Figure 6b). This is a larger decrease than we measured for air-filled porosity at a matric potential of −10 kPa corresponding to pores with an equivalent diameter of 30 µm (Supplemental Figure S2), indicating that large macropores were more affected by compaction than smaller macropores. Percolating porosity and connectivity decreased by 60–90% due to compaction (Figure 6b), illustrating that compaction had adverse impacts on pore connectivity. Compaction also caused a strong reduction in critical pore diameter (Figure 6b), contributing to the decline in air permeability (Figure 4) and saturated hydraulic conductivity (Supplemental Figure S4). Macropore properties obtained from x-ray imaging were strongly correlated with fluid transport properties ($r = .45$–$.78$; Supplemental Table S6). These results indicate a strong negative effect of compaction on large pores and their connectivity, resulting in stronger decrease of fluid transport properties than air-filled or total porosity (Figures 3 and 4; Supplemental Figures S2–S4).

The improvement of macroporosity, critical pore diameter, percolating porosity, and connectivity with time after compaction (Figure 6b) indicates signs of structural recovery, although differences between sampling times were not

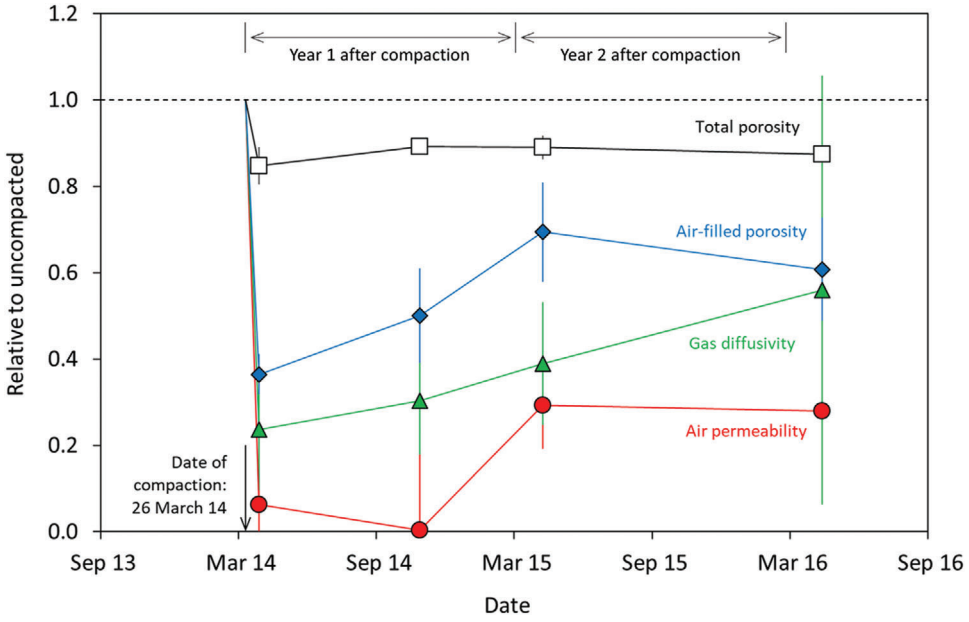

FIGURE 5 Different soil physical properties are differently affected by compaction (c.f., data some days after compaction) and recover at different rates. The figure shows relative values of the compacted plots (noncompacted = 1.0) for total porosity, air-filled porosity, gas diffusivity, and air permeability of the ley treatment at 0.1 m depth. Error bars represent SE ($n = 3$)

statistically significant ($p > .05$) due to relatively high local variability (Supplemental Table S3). Similar to porosity and fluid transport properties (previous section), we found no significant change with time for any of the measured properties (Supplemental Table S3), and we found nonsignificant differences between compacted and noncompacted soil 2 yr after compaction (Supplemental Table S6), indicating recovery trends. The high correlations between macropore characteristics and gas transport properties (Supplemental Table S8) indicate that the re-creation of a connected macropore system is crucial for the improvement of fluid transport properties. We therefore suggest that the creation of new macropores in an initially compacted bulk soil plays an important role in the recovery of gas and water transport properties, and hypothesize that this promotes the progression of the recovery front from pockets (hotspots) into the bulk soil, as discussed below.

3.4 | Soil moisture and aeration conditions in the soil profile

Figure 8 illustrates impacts of deteriorated gas and water transport properties on O_2 concentration levels in soil air and on soil water contents. The reduced gas transport capability of the compacted soil (Figure 4; Supplemental Figure S3) reduced O_2 concentrations in the topsoil (not shown) and the subsoil (Figure 8a). Oxygen concentrations as low as 5% were measured in the compacted treatments in the first 2–3 mo (spring) after the compaction event.

Compaction resulted in generally lower soil water contents, which was particularly pronounced in the ley treatment (Figure 8b). The control (no compaction) treatments tended to wet more gradually following rainfall (c.f., the slope of the increase in water content of the compacted vs. control ley in the beginning of November 2016 in Figure 8b). Bare soil remained wetter compared with soil under ley due to the absence of water uptake by vegetation (Figure 8b).

3.5 | Earthworm biomass

Earthworm biomass for the three classical ecological groups is presented in Table 1. Total earthworm biomass was about 2,000 kg per hectare in the noncompacted ley, except in 2015 when only ~600 kg of earthworms were found. This could be due to unfavorably dry conditions during sampling in 2015 (or other unknown temporal variation). The compaction event in spring 2014 significantly reduced ($p < .05$) total earthworm biomass to about one-third of the precompaction population. The relative decline in earthworm abundance was similar for epigeic and endogeic earthworms, whereas anecic earthworms were slightly less affected by compaction (Table 1).

The ratio of earthworm biomass of the compacted to the control treatment increased slightly in the ley (to about 56%) but remained very low for the bare soil (only 13% biomass in compacted relative to control) 1 yr after compaction (2015; Table 1). In that same year we measured the highest earthworm biomass in the bare soil control treatment. We interpret this observation as indicating temporally ideal conditions in

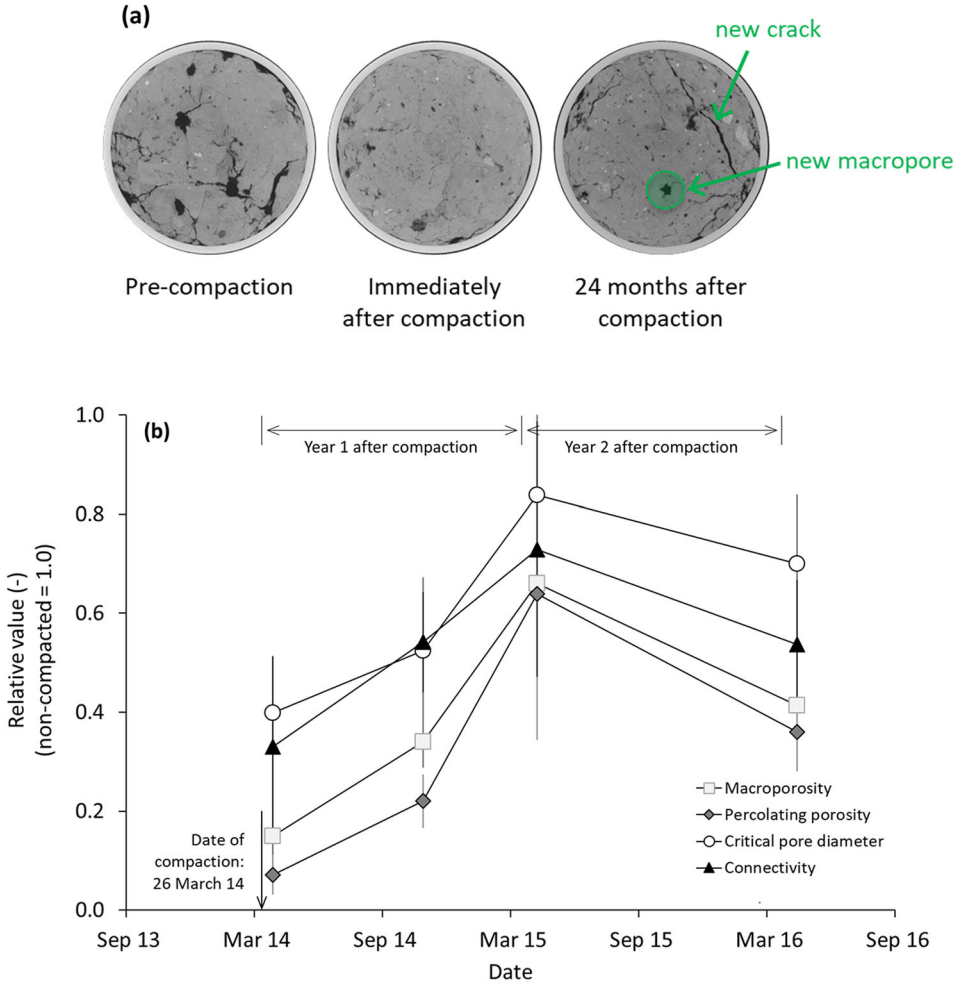

FIGURE 6 Quantification of soil pore system using computed tomography imaging (pores >120 μm, based on voxel size of 60 μm). (a) Illustrative examples of cross sections through soil cores, and (b) evolution of macropore characteristics (plotted as relative values, noncompacted = 1.0) of the ley treatment at 0.1 m depth. Error bars in (b) represent SE ($n = 3$)

TABLE 1 Earthworm biomass in kg ha^{-1}

				2015				2016			
	2013	2014		Control		Compacted		Control		Compacted	
Variable	Precompaction	Control	Compacted	Ley	Bare soil	Ley	Bare soil	Ley	Bare soil	Ley	Bare soil
Ecological group											
Epigeic	107	115	35	8	13	45	0	139	70	116	2
Endogeic	499	476	155	197	278	76	80	492	436	286	266
Anecic	1,581	1,484	605	394	599	217	32	1,205	820	936	828
Total biomass	2,187	2,075	794	600	890	338	112	1,836	1,326	1,337	1,096

Note. In 2014, earthworms were sampled shortly after the compaction event and therefore only distinguish control and compacted soil, as the duration of the ley vs. bare soil treatments was too short to show any effect.

the bare soil (high soil moisture, e.g., Figure 8b; with sufficient C food resources in the soil from decomposed plant material). In spring 2016, 2 yr after the compaction event, earthworm biomass in compacted plots were 73–83% but not significantly lower ($p > .05$) than those in control plots, and the total biomass in the bare soil treatments were lower than in the ley, although not at a significant level ($p > .05$) (Table 1; Supplemental Table S7).

From the sampling of earthworm casts at the soil surface, we estimated an excretion rate at the soil surface of about 1.5 kg m^2 yr^{-1} (of soil). Slightly higher egestion rates were estimated for bare soil than for the ley treatment.

4 | DISCUSSION

An important observation stemming from this study is that different soil physical properties follow different recovery paths and rates (Figures 3 and 4; Supplemental Figures S2–S4). In general, soil physical properties have not fully recovered to precompaction values within 2 yr after compaction as seen in our measurements (Figures 3–6; Supplemental Figures S2–S4) and supported from observations of ponding water after large rainfall events (Figure 1d). Previous studies have reported that compaction could persist for decades (for an overview, see Keller et al., 2017 and references therein). Notably, our data demonstrate that natural recovery is slow also within the topsoil (0.1 m depth), whereas many previous studies reporting persistency of compaction focused on tilled soil (Arvidsson & Håkansson, 1996; Besson et al., 2013; Weisskopf et al., 2010) or on subsoil (Berisso et al., 2012; Håkansson et al., 1988; Peng & Horn, 2008).

We were unable to discern differences in recovery of soil physical properties between the ley and the bare soil treatment after 2 yr, contrary to expectation that biological activity with plants would promote soil functional recovery. Root decay in the bare soil may have contributed to the formation of new pore spaces for transport of water and air. Part of this lack of difference is possibly also attributed to sufficient quantities of residual soil organic C in the bare soil after compaction that supported burrowing activity at levels not yet hindered by available soil organic C (energy source). Similar initial increases in surface infiltration in the bare soil and ley treatments (April–Novembers 2014; Figure 2) support this argument, although shrinkage cracks induced by surface drying during summer may have also contributed to the increase in surface infiltration. During winter, recovery was retarded in the bare soil treatments (Figure 2), possibly by surface slaking and seal formation (Figure 1c), which was observed to occur during periods of rapid snowmelt. Surface slaking in bare soil may also result in downward transport of soil particles causing pore clogging (Le Bissonnais, 2010; Yang et al., 2020); indeed, data from our last sampling date 2 yr after compaction may indicate the onset of soil structure degradation in the bare soil control plots (Figures 2–4). The different management by compaction combinations resulted in certain differences in soil conditions, but the interactions are complex. Oxygen concentrations in soil air were generally low in the ley independent of compaction level and higher in the noncompacted bare soil, which is likely due to higher biological activity in ley during summer months (Figure 7a). The presence or absence of vegetation had a stronger control on soil moisture than compaction (Figure 7b). Water contents were generally lower in compacted soil, especially in ley (Figure 7b), which could be explained by reduced water infiltration capacity and saturated hydraulic conductivity (Figure 2; Supplemental Figure S4), increased unsaturated hydraulic conductivity (Richard et al., 2001), and increased evaporative length (i.e., greater depth at which evaporation occurs) in compacted soil (Or & Lehmann, 2019), and, for ley, a shallower root system in compacted soil due to increased penetration resistance (Supplemental Figure S5; Colombi et al., 2018).

4.1 | Postcompaction recovery rates differ among soil properties

Soil properties that were most strongly affected by soil compaction displayed trends of recovery. The soil total porosity was reduced by about 15% due to compaction but did not change much during the first 2 yr after compaction, whereas air permeability, which reduced by almost two orders of magnitude, has shown signs of recovery 1 yr after compaction (Figure 5). However, we note the bias in our ability to detect recovery from compaction that is greater for a property that exhibited a larger change due to compaction than a property that was not strongly affected by compaction. Nevertheless, different recovery rates for different soil physical properties are expected because of differences in sensitivity to small changes in soil pore features.

Because different soil properties are governed by distinct soil pore characteristics (porosity, connectivity, critical pore diameter), recovery rates vary between soil properties. This also implies that different recovery processes (root growth, earthworm bioturbation, shrink–swell and freeze–thaw cycles) affect different soil properties in different ways and magnitudes. We found a relatively fast recovery of air permeability within the first year after compaction, but little further change during the second year after compaction (Figure 5). Air permeability and saturated hydraulic conductivity are governed by the largest continuous pores and critical pore diameter (i.e., the bottleneck) (Berli et al., 2008; Koestel et al., 2018). Therefore, destruction or distortion of large pores by compaction (Figure 6) dramatically reduces air permeability and saturated hydraulic conductivity. Conversely, a new macropore, created by an earthworm or a plant root, can considerably increase permeability. This is supported by strong correlations between macropore characteristics and air permeability and saturated hydraulic conductivity, respectively (Supplemental Table S8). The temporal evolution of air permeability (Figure 5) was closely linked to the evolution of macropore characteristics (Figure 6b). We hypothesize that recovery rates of properties that are largely dependent on pore size (critical pore diameter) such as permeability show a stepwise recovery, whereas properties that are less sensitive to specific pore sizes (e.g., gas diffusivity) show more gradual changes. This makes recovery rates of pore-size dependent properties difficult to predict because they involve a

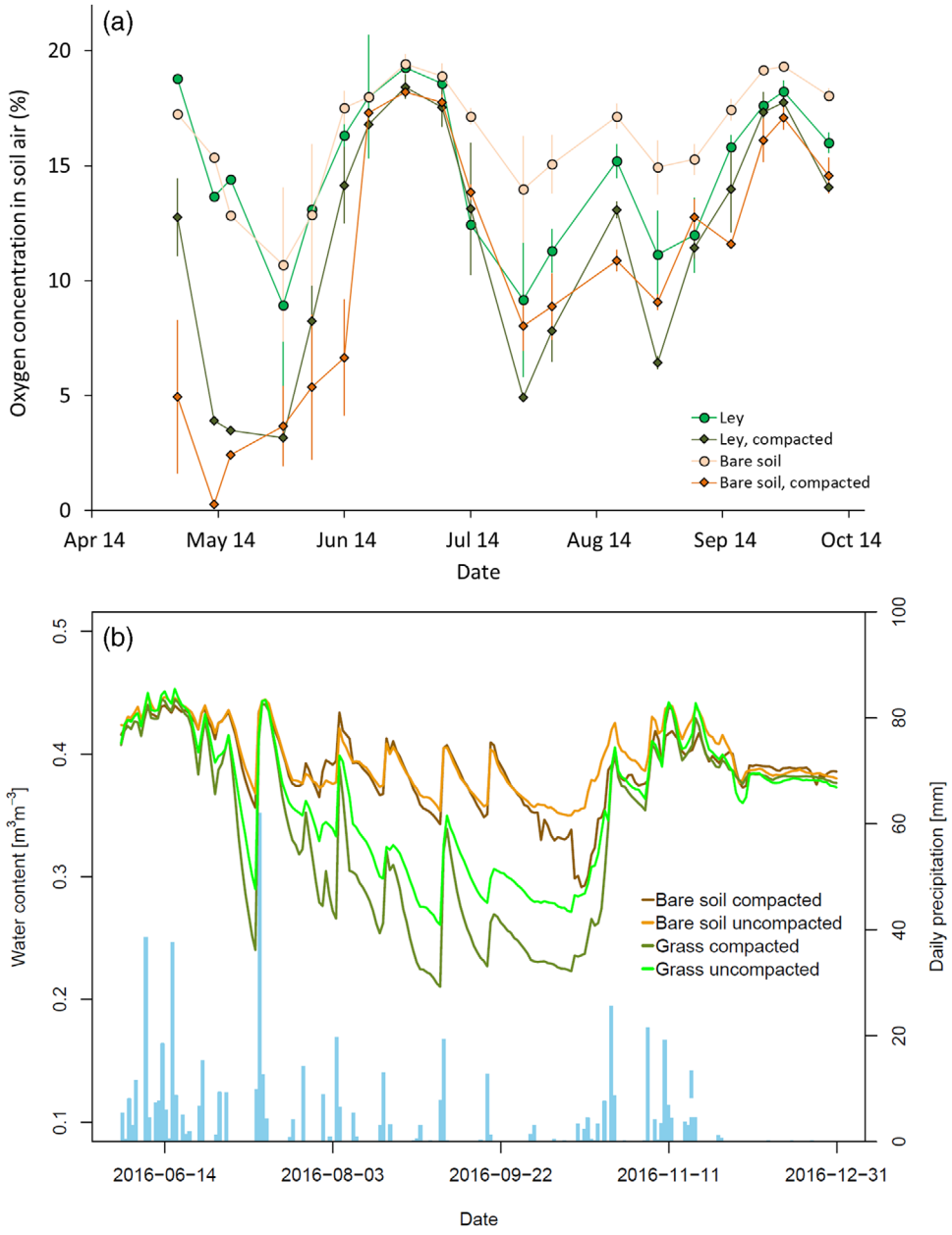

FIGURE 7 Illustrative examples of compaction-induced deteriorated fluid transport properties on soil conditions: (a) O_2 concentration at 0.4 m depth in the first year after compaction (error bars represent SE, $n = 2$ experimental blocks), and (b) soil water content at 0.1 m depth in the third year after compaction ($n = 2$)

stochastic component: would, for example, an earthworm burrow through exactly this location in the soil or not?

4.2 | Recovery of total porosity requires net upward movement of soil particles and internal bulk volume expansion

Several biotic and abiotic processes could improve soil structure, thereby contributing to recover soil functions following compaction, but not all of these processes promote soil decompaction (Table 2). We have to distinguish between soil structure and function improvement (induced by a change in pore size distribution and pore connectivity without a change in total pore volume) and bulk soil decompaction (i.e., pore volume increase). Soil compaction is accompanied with downward movement of soil particles, but recovery of macroporosity following compaction does not necessarily involve upward movement of soil. In other words, compaction and recovery of soil structure and function do not necessarily happen along the same pathways, as also evidenced from our data (e.g., Figure 5).

TABLE 2 Biotic and abiotic processes of soil structure recovery following compaction

Recovery process	Excavation/soil expansion rate	Persistence, legacy/remarks	References
Biotic decompacting processes			
Burrowing by anecic earthworms	10–50 Mg ha^{-1} yr^{-1}	burrows can exist for years	1,2,3
Burrowing ants	1–5 Mg ha^{-1} yr^{-1}	nests exist for years	3
Burrowing termites	1–5 Mg ha^{-1} yr^{-1}	nests exist for years, termites restricted to tropical regions	3
Burrowing invertebrates (e.g., beetles)	<1 Mg ha^{-1} yr^{-1}	limited knowledge on persistence	3
Burrowing by ground-nesting wild bees, wasps	1–5 Mg ha^{-1} yr^{-1}	limited knowledge on persistence of burrows	4,5
Burrowing by mammals	1–5 Mg ha^{-1} yr$^{-1\dagger)}$	burrows can exist for years, little considered in the context of soil structure evolution, considered a pest on arable fields	3
Soil uplifting by root heave	[a]	not enough knowledge	
Biotic processes, no net volume change			
Bioturbation by endogeic earthworms	–	weeks to months (seasonal)	2
Biopore formation by roots	–	root channels persist for years	6
Abiotic processes: potential net volume change but little quantitative information on expansion rates			
Soil viscoelastic rebound	[b]	elastic rebound instantaneous, limited knowledge about rebound after compaction at profile scale	7
Drying-induced shrinkage (shrink–swell cycles)	[b]	seasonal: cracks close upon wetting, planes of weaknesses can remain, microstructural changes needed to result in net volume change	8
Freezing (freeze–thaw cycles with ice lens formation)	[b]	can both increase or decrease porosity, impact on porosity depending on initial conditions and freezing characteristics	9

Note. Only some processes involve upward movement of soil particles or soil expansion and therefore effectively decompact the soil, whereas others improve soil structure and function through modification of soil pore size distribution without changing overall (total) porosity. Typical excavation (mounding) rates are given for decompacting processes.

[a]Not enough knowledge, soil uplift rate as well as depth of influence are presumably small.

[b]Not enough knowledge to give quantitative information on expansion rates.

References: 1) Edwards and Bohlen (1996); 2) Lee (1985); 3) Wilkinson et al. (2009); 4) Watanabe (1998); 5) Michener (2007); 6) Watt et al. (2006); 7) Or and Ghezzehei (2002); 8) Dexter (1991); 9) Viklander (1998).

Soil volume expansion could occur due to wetting-induced swelling of active clay minerals (Arthur et al., 2013; Tessier, 1990; Tuller & Or, 2003) during certain freeze–thaw processes with formation of ice lenses (Qi et al., 2006), or in the form of viscoelastic rebound after removing a load (Or & Ghezzehei, 2002), but we are not aware of quantitative information on expansion rates following compaction (Table 2). Shrinking and swelling can play an important role in improving structure and function of soils containing expansive clay minerals. Drying-induced soil shrinkage forms desiccation cracks, which serve as pathways for water, air, and roots, and increase the accessible surface area, thereby facilitating the progression of recovery fronts as discussed below. Drying is not only induced by climatic forces, plants play an important role in drying soil (Figure 7b), especially at larger soil depths. Shrinkage and swelling may appear as similar processes but with opposite directions, suggesting no overall change in total porosity upon repeated drying–wetting cycles (Diel et al., 2019). However, changes in microstructure (i.e., particle rearrangement) may occur during drying–shrinkage or wetting–swelling (Tessier, 1990), which could result in an increase in total porosity. Freeze–thaw cycles can increase or decrease total porosity due to microstructural changes (Qi et al., 2006; Viklander, 1998). However, freeze–thaw effects play a small role and only affected shallow soil depths at our experimental site due to the generally mild winters (Supplemental Figure S1).

Decompaction by removing of soil from a given volume occurs by burrowing of fauna. Typical excavation rates are indicated in Table 2. Whereas burrowing by earthworms (in

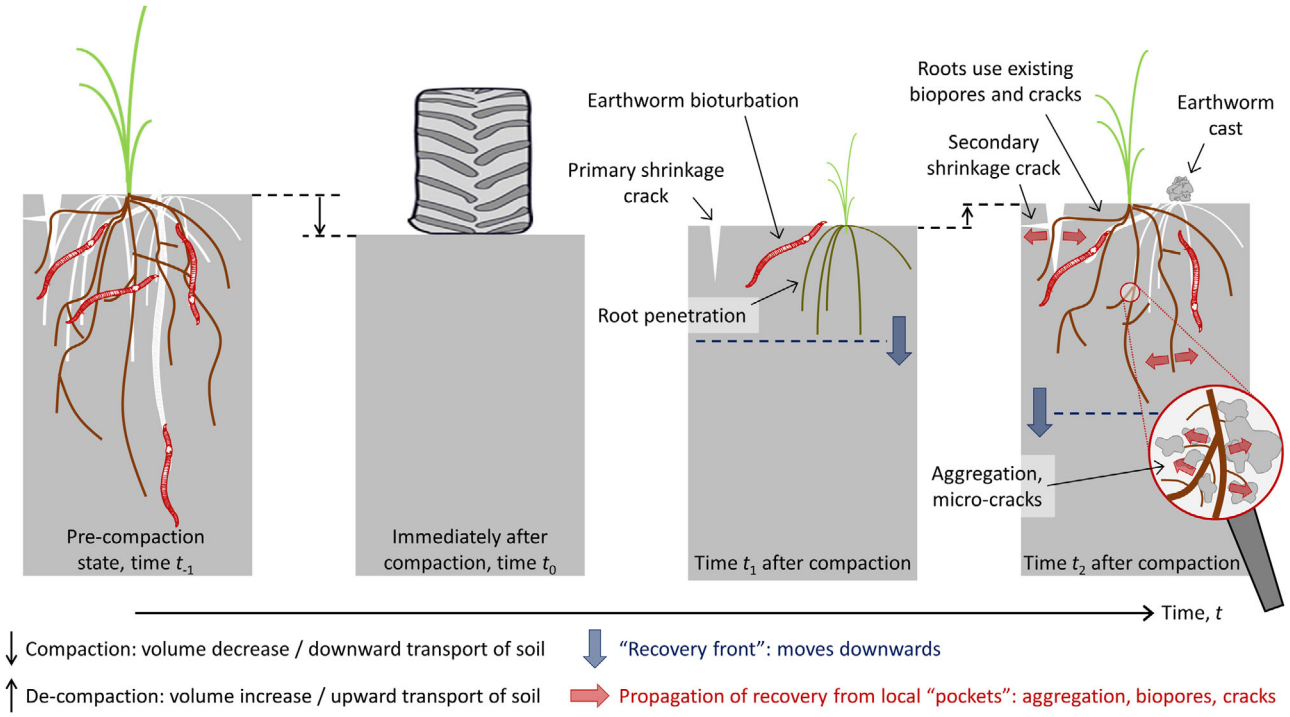

FIGURE 8 Conceptual figure of natural soil structure recovery after compaction. There are two recovery fronts, one progressing from the soil surface downward, and one progressing from local pockets (such as biopores) to the bulk soil

temperate regions) and termites (in tropical areas) are well recognized, less is known about impacts on soil structure evolution and rates of soil excavation of ants, ground-nesting flying insects, birds, or mammals, and their contribution to soil structure evolution. Despite many beneficial contributions to soil structure, not all earthworms decompact the bulk soil (Table 2). Only those earthworms that ingest soil and lay cast at the soil surface are likely to contribute to soil decompaction at the soil profile scale. Earthworms that excrete casts within the soil may change local bulk density but not overall porosity at the profile scale. Considerable earthworm activity is needed before changes in total porosity or bulk density become detectable. The estimated excretion rate of 1.5 kg m^2 yr^{-1} (corresponding to 15 Mg ha^{-1} yr^{-1}) for the experiment is well within estimates of egestion rates reported in the literature (Table 2). Assuming a depth of bioturbation of 0.5 m (Jarvis et al., 2010) and taking an average bulk density of 1.5 Mg m^{-3} of the 0–0.5-m depth (Figure 3) suggests a decrease in bulk density of only about 0.005 Mg m^{-3} per year (from 1.5 to 1.495 Mg m^{-3}). This negligible decrease in bulk density is consistent with our observations that bulk density did not recover in the first 2 yr following compaction (Figure 3). Even for an assumed excretion rate of 10 kg m^2 yr^{-1}, a maximum reported by Edwards and Bohlen (1996) for temperate grassland, the associated decrease in soil bulk density is only 0.02 Mg m^{-3} per year. Considering the observed increase of 0.15–0.20 Mg in bulk density due to compaction, recovery would take at least a decade for bulk porosity recovery to precompaction state.

Growing plant roots often modify pore size distribution by forming biopores without altering total porosity, because roots push soil radially within a fixed soil volume (Dexter, 1987a). Consequently, plant root growth does not result in decompaction of bulk soil as indicated in Table 2. Moreover, evidence suggests that growing roots preferentially use existing macropores as far as possible resulting in a limited number of new macropores, especially in compacted soil (Colombi et al., 2017; Cresswell & Kirkegaard, 1995; Dexter, 1986; Or et al., 2021; Watt et al., 2006). Although we have not attempted to separate pores created by roots or earthworms in our analysis here, results show that macroporosity increased after compaction (Figure 6), which improved fluid transport properties with nearly no changes in total porosity (Figure 5). We note that the potential to modify soil structure differs between plant species (Bengough et al., 2011; Helliwell et al., 2019; Muhandiram et al., 2020). A potential mechanism involving root growth that would contribute to increasing total porosity is upward lifting of soil via root heave as exemplified with tree root growth (Philips & Marion, 2006), but it is unknown whether a similar process occurs in arable crops and ley with much finer roots (Table 2). Presumably, the impact would be limited to a shallow soil layer.

4.3 | Structural recovery progresses from the soil surface downwards and internally expands from pockets (hotspots) to bulk soil

Based on observations of this study and considerations discussed above, we deduce a conceptual framework for soil structure recovery after compaction. We propose that recovery progresses along two recovery fronts (Figure 8): one that progresses from the soil surface downward, and one that progresses from local pockets to bulk soil (i.e., into compacted soil volumes). Progression from the soil surface downward is motivated by a decreasing exposure to climatic forces and decreasing biological activity with increasing distance from the soil surface, a conclusion supported by our findings that soil physical properties quickly recovered at the soil surface (Figure 2) but not at greater depths (Figures 4–6; Supplemental Figure S2–S4). Progression from pockets to bulk soil implies that newly created pore volumes (biopores, shrinkage cracks) act as hotspots for biological activity (including soil aggregation and water uptake-induced shrinkage), providing access points for preferential expansion of pore spaces by roots and earthworms. The observed increase in macroporosity and macropore connectivity after compaction (Figure 6) indicate the development of such pockets, and we hypothesize that these pockets facilitate the further propagation of recovery into still compacted soil volumes. Additional data of longer time series at our site as well as other sites will be needed to obtain experimental evidence of recovery progression from pockets to bulk soil. The concept of facilitative fronts for soil structure recovery is supported by the role of strategic tillage for accelerating soil structure recovery under no-till as discussed by Conyers et al. (2019). Detailed discussion of such facilitative processes will be explored in a future study.

5 | CONCLUSIONS

Measurements at our field site show that soil physical properties have not recovered to precompaction levels within 2 yr after a severe compaction, even in the topsoil. We found no difference between a treatment with (ley) and without vegetation (bare soil), presumably because the period of 2 yr after compaction in this study was too short to induce (and identify) differences. We expect that continued monitoring can reveal further distinctions between the management treatments and allow us to better elucidate the relevant recovery rates and associated time scales for respective soil physical properties. Postcompaction recovery rates tended to decrease with depth, are not constant over time, and differ between soil properties. Our data indicate that properties that were most severely affected by compaction, such as air permeability and saturated hydraulic conductivity, are the properties with trends of recovery. In contrast, no recovery trend was measured for bulk density and total porosity. This is because an increase in total porosity requires upward transport of soil, whereas permeability can be increased by creation of a new macropore that does not require an increase in total porosity. Based on our observations and considerations, we suggest that recovery proceeds at two fronts, from the surface downward and from local pockets to the bulk soil. Top-down progression of the recovery front is explained by decreasing exposure to climatic forces and decreasing biological activity with depth. Recovery proceeding from local pockets to the bulk soil implies that newly created pore volumes (biopores, desiccation cracks) may act as local hotspots of biological activity and facilitate further progression of earthworm burrowing, root proliferation, and drying-induced shrinkage. Validation of this concept requires additional data of longer time series, as well as measurements in other soils and climates.

ACKNOWLEDGMENTS

Financial support from the Swiss National Science Foundation (SNSF) through the National Research Program 68 "Soil Resources" is gratefully acknowledged (Project no. 406840-143061). SJS is supported by the Luxembourg National Research Fund (FNR) ATTRACT programme (A16/SR/11254288). Dr. Peter Lehmann (ETH Zürich, Soil and Terrestrial Environmental Physics) is thanked for performing the randomization of sampling locations. Many present and former members of our research groups at Agroscope Zürich (Soil Quality and Soil Management) and ETH Zürich (Soil and Terrestrial Environmental Physics, and Crop Science), and present and former members of Agroscope support groups (Field Trial Support, Mechanical Workshop, and Electronics Workshop) are thanked for their invaluable help with soil sampling, design and installation of sensor probes, field measurements, and farming operations.

AUTHOR CONTRIBUTIONS

Thomas Keller, Conceptualization, Data curation, Formal analysis, Funding acquisition, Investigation, Methodology, Project administration, Writing-original draft, Writing-review and editing; Tino Colombi, Conceptualization, Formal analysis, Investigation, Methodology, Writing-original draft, Writing-review and editing; Siul Ruiz, Formal analysis, Investigation, Writing-review and editing; Stan Schymanski, Funding acquisition, Investigation, Methodology, Writing-review and editing; Peter Weisskopf, Funding acquisition, Investigation, Methodology, Writing-review and editing; John Koestel, Formal analysis, Writing-review and editing; Marlies Sommer, Formal analysis, Investigation, Methodology; Viktor Stadelmann, Investigation, Methodology; Dani Breitenstein, Investigation, Methodology; Norbert Kirchgessner, Investigation, Methodology, Writing-review and editing; Achim Walter, Funding acquisition, Writing-review and

editing; Dani Or, Conceptualization, Funding acquisition, Investigation, Methodology, Writing-original draft, Writing-review and editing.

CONFLICT OF INTEREST

Authors declare no conflicts of interest.

ORCID

Thomas Keller https://orcid.org/0000-0002-9383-3209
Tino Colombi https://orcid.org/0000-0001-8493-4430
Siul Ruiz https://orcid.org/0000-0002-6273-8516
Stanislaus J. Schymanski https://orcid.org/0000-0002-0950-2942
Peter Weisskopf https://orcid.org/0000-0003-4952-174X
John Koestel https://orcid.org/0000-0002-3230-5699
Norbert Kirchgessner https://orcid.org/0000-0001-8517-6555
Achim Walter https://orcid.org/0000-0001-7753-9643
Dani Or https://orcid.org/0000-0002-3236-2933

REFERENCES

Arthur, E., Moldrup, P., Schjønning, P., & de Jonge, L. W. (2013). Water retention, gas transport, and pore network complexity during short-term regeneration of soil structure. *Soil Science of America Journal*, *77*, 1965–1976. https://doi.org/10.2136/sssaj2013.07.0270

Arthur, E., Schjønning, P., Moldrup, P., & de Jonge, L. W. (2012). Soil resistance and resilience to mechanical stresses for three differently managed sandy loam soils. *Geoderma*, *173–174*, 50–60. https://doi.org/10.1016/j.geoderma.2012.01.007

Arvidsson, J., & Håkansson, I. (1996). Do effects of soil compaction persist after ploughing? Results from 21 long-term field experiments in Sweden. *Soil & Tillage Research*, *39*, 175–197.

Barzegar, A. R., Rengasamy, P., & Oades, J. M. (1995). Effect of clay type and rate of wetting on the mellowing ratio of compacted soils. *Geoderma*, *68*, 39–49. https://doi.org/10.1016/0016-7061(95)00022-G

Beck-Broichsitter, S., Gerke, H. H., Leue, M., von Jeetze, P., & Horn, R. (2020). Anisotropy of unsaturated soil hydraulic properties of eroded Luvisol after conversion to hayfield comparing alfalfa and grass plots. *Soil & Tillage Research*, *198*, 104553.

Bengough, A. G., McKenzie, B. M., Hallett, P. D., & Valentine, T. A. (2011). Root elongation, water stress, and mechanical impedance: A review of limiting stresses and beneficial root tip traits. *Journal of Experimental Botany*, *62*, 59–68. https://doi.org/10.1093/jxb/erq350

Besson, A., Séger, M., Giot, G., & Cousin, I. (2013). Identifying the characteristic scales of soil structural recovery after compaction from three in-field methods of monitoring. *Geoderma*, *204–205*, 130–139. https://doi.org/10.1016/j.geoderma.2013.04.010

Berisso, F. E., Schjønning, P., Keller, T., Lamandé, M., Etana, A., de Jonge, L. W., Iversen, B. V., Arvidsson, J., & Forkman, J. (2012). Persistent effects of subsoil compaction on pore characteristics and functions in a loamy soil. *Soil & Tillage Research*, *122*, 42–51.

Berli, M., Carminati, A., Ghezzehei, T. A., & Or, D. (2008). Evolution of unsaturated hydraulic conductivity of aggregated soils due to compressive forces. *Water Resources Research*, *44*, W00C09. https://doi.org/10.1029/2007WR006501

Berli, M., Kulli, B., Attinger, W., Keller, M., Leuenberger, J., Flühler, H., Springman, S. M., & Schulin, R. (2004). Compaction of agricultural and forest subsoils by tracked heavy construction machinery. *Soil & Tillage Research*, *75*, 37–52.

Blackwell, P. S., Ward, M. A., Lefevre, R. N., & Cowand, D. J. (1985). Compaction of a swelling clay soil by agricultural traffic: Effects upon conditions for growth of winter cereals and evidence for some recovery of structure. *Journal of Soil Science*, *36*, 633–650. https://doi.org/10.1111/j.1365-2389.1985.tb00365.x

Bouwman, L. A., & Arts, W. B. M. (2000). Effects of soil compaction on the relationships between nematodes, grass production and soil physical properties. *Applied Soil Ecology*, *14*, 213–222. https://doi.org/10.1016/S0929-1393(00)00055-X

Brus, D. J., & van den Akker, J. J. H. (2018). How serious a problem is subsoil compaction in the Netherlands? A survey based on probability sampling. *SOIL*, *4*, 37–45. https://doi.org/10.5194/soil-4-37-2018

Buckingham, E. (1904). Contributions to our knowledge of the aeration of soils. *USDA Bureau of Soils Bulletin*, *25*, U.S. Government Printing Office.

Colombi, T., Braun, S., Keller, T., & Walter, A. (2017). Artificial macropores attract crop roots and enhance productivity on compacted soils. *Science of the Total Environment*, *574*, 1283–1293. https://doi.org/10.1016/j.scitotenv.2016.07.194

Colombi, T., Torres, L. C., Walter, A., & Keller, T. (2018). Feedbacks between soil penetration resistance, root architecture and water uptake limit water accessibility and crop growth– a vicious circle. *Science of the Total Environment*, *626*, 1026–1035. https://doi.org/10.1016/j.scitotenv.2018.01.129

Conyers, M., van der Rijt, V., Oates, A., Poile, G., Kirkegaard, J., & Kirkby, C. (2019). The strategic use of minimum tillage within conservation agriculture in southern New South Wales, Australia. *Soil & Tillage Research*, *193*, 17–26.

Cresswell, H. P., & Kirkegaard, J. A. (1995). Subsoil amelioration by plant-roots – the process and the evidence. *Soil Research*, *33*, 221–239. https://doi.org/10.1071/SR9950221

de Mendiburu, F. (2017). Agricolae: Statistical procedures for agricultural research. https://cran.r-project.org/web/packages/agricolae/

DeArmond, D., Emmert, F., Lima, A. J. N., & Higuchi, N. (2019). Impacts of soil compaction persist 30 years after logging operations in the Amazon Basin. *Soil & Tillage Research*, *189*, 207–216.

Dexter, A. R. (1986). Model experiments on the behaviour of roots at the interface between a tilled seed-bed and a compacted sub-soil, III. Entry of pea and wheat roots into cylindrical biopores. *Plant and Soil*, *95*, 149–161. https://doi.org/10.1007/BF02378860

Dexter, A. R. (1987a). Compression of soil around roots. *Plant and Soil*, *97*, 401–406. https://doi.org/10.1007/BF02383230

Dexter, A. R. (1987b). Mechanics of root growth. *Plant and Soil*, *98*, 303–312. https://doi.org/10.1007/BF02378351

Dexter, A. R. (1991). Amelioration of soil by natural processes. *Soil & Tillage Research*, *20*, 87–100.

Diel, J., Vogel, H. J., & Schlüter, S. (2019). Impact of wetting and drying cycles on soil structure dynamics. *Geoderma*, *345*, 63–71. https://doi.org/10.1016/j.geoderma.2019.03.018

Doube, M., Klosowski, M. M., Arganda-Carreras, I., Cordelieres, F. P., Dougherty, R. P., Jackson, J. S., Schmid, B., Hutchinson, J. R., & Shefelbine, S. J. (2010). BoneJ Free and extensible bone image analysis in ImageJ. *Bone*, *47*, 1076–1079. https://doi.org/10.1016/j.bone.2010.08.023

Edwards, C. A., & Bohlen, P. (1996). *Biology and ecology of earthworms*. Chapman & Hall.

Goutal, N., Boivin, P., & Ranger, J. (2012). Assessment of natural recovery rate of soil specific volume following forest soil compaction. *Soil Science Society of America Journal*, *76*, 1426–1435. https://doi.org/10.2136/sssaj2011.0402

Graves, A. R., Morris, J., Deeks, L. K., Rickson, R. J., Kibblewhite, M. G., Harris, J. A., Farewell, T. S., & Truckle, I. (2015). The total costs of soil degradation in England and Wales. *Ecological Economics*, *119*, 399–413. https://doi.org/10.1016/j.ecolecon.2015.07.026

Greenwood, K. L., & McKenzie, B. M. (2001). Grazing effects on soil physical properties and the consequences for pastures. *Australian Journal of Experimental Agriculture*, *41*, 1231–1250. https://doi.org/10.1071/EA00102

Gregory, A. S., Watts, C. W., Griffiths, B. S., Hallett, P. D., Kuan, H. L., & Whitmore, A. P. (2009). The effect of long-term soil management on the physical and biological resilience of a range of arable and grassland soils in England. *Geoderma*, *153*, 172–185. https://doi.org/10.1016/j.geoderma.2009.08.002

Gregory, A. S., Watts, C. W., Whalley, W. R., Kuan, H. L., Griffiths, B. S., Hallett, P. D., & Whitmore, A. P. (2007). Physical resilience of soil to field compaction and the interactions with plant growth and microbial community structure. *European Journal of Soil Science*, *58*, 1221–1232. https://doi.org/10.1111/j.1365-2389.2007.00956.x

Helliwell, J. R., Sturrock, C. J., Miller, A. J., Whalley, W. R., & Mooney, S. J. (2019). The role of plant species and soil condition in the structural development of the rhizosphere. *Plant Cell and Environment*, *42*, 1974–1986. https://doi.org/10.1111/pce.13529

Håkansson, I., Voorhees, W. B., & Riley, H. (1988). Vehicle and wheel factors influencing soil compaction and crop response in different traffic regimes. *Soil & Tillage Research*, *11*, 239–282.

Horn, R., Domżżał, H., Słowińska-Jurkiewiecz, A., & van Owerkerk, C. (1995). Soil compaction processes and their effects on the structure of arable soils and the environment. *Soil & Tillage Research*, *35*, 23–36.

IUSS Working Group WRB. (2015). World reference base for soil resources 2014: International soil classification system for naming soils and creating legends for soil maps (update 2015, World Soil Resources Reports No. 106). FAO.

Jarvis, N., Larsbo, M., & Koestel, J. (2017). Connectivity and percolation of structural pore networks in a cultivated silt loam soil quantified by X-ray tomography. *Geoderma*, *287*, 71–79. https://doi.org/10.1016/j.geoderma.2016.06.026

Jarvis, N. J., Taylor, A., Larsbo, M., Etana, A., & Rosén, K. (2010). Modelling the effects of bioturbation on the re-distribution of ^{137}Cs in an undisturbed grassland soil. *European Journal of Soil Science*, *61*, 24–34. https://doi.org/10.1111/j.1365-2389.2009.01209.x

Jones, S. B., Wraith, J. M., & Or, D. (2002). Time domain reflectometry (TDR) measurement principles and applications. *Hydrological Processes*, *16*, 141–153. https://doi.org/10.1002/hyp.513

Keller, T., Colombi, T., Ruiz, S., Manalili, M. P., Rek, J., Stadelmann, V., Wunderli, H., Breitenstein, D., Reiser, R., Oberholzer, H. - R., Schymanski, S., Romero-Ruiz, A., Linde, N., Weisskopf, P., Walter, A., & Or, D. (2017). Long-term soil structure observatory for monitoring post-compaction evolution of soil structure. *Vadose Zone Journal*, *16*(4). https://doi.org/10.2136/vzj2016.11.0118

Keller, T., Sandin, M., Colombi, T., Horn, R., & Or, D. (2019). Historical increase in agricultural machinery weights enhanced soil stress levels and adversely affected soil functioning. *Soil & Tillage Research*, *194*, 104293. https://doi.org/10.1016/j.still.2019.104293

Kissling, M., Hegetschweiler, K. T., Rusterholz, H. - P., & Baur, B. (2009). Short-term and long-term effects of human trampling on above-ground vegetation, soil density, soil organic matter and soil microbial processes in suburban beech forests. *Applied Soil Ecology*, *42*, 303–314. https://doi.org/10.1016/j.apsoil.2009.05.008

Klute, A., & Dirksen, C. (1986). Hydraulic conductivity and diffusivity: Laboratory methods. In A. Klute (Ed.), *Methods of soil analysis, Part 1*, (pp. 687–732, 2nd ed.). SSSA Book Series 5, SSSA and ASA.

Koestel, J. (2018). SoilJ: An ImageJ plugin for the semiautomatic processing of three-dimensional X-ray images of soils. *Vadose Zone Journal*, *17*. https://doi.org/10.2136/vzj2017.03.0062

Koestel, J., Dathe, A., Skaggs, T. H., Klakegg, O., Ahmad, M. A., Babko, M., Giménez, D., Farkas, C., Nemes, A., & Jarvis, N. (2018). Estimating the permeability of naturally structured soil from percolation theory and pore space characteristics imaged by X-ray. *Water Resources Research*, *54*, 9255–9263. https://doi.org/10.1029/2018WR023609

Koestel, J., & Schlüter, S. (2019). Quantification of the structure evolution in a garden soil over the course of two years. *Geoderma*, *338*, 597–609. https://doi.org/10.1016/j.geoderma.2018.12.030

Kramer, S., Weisskopf, P., & Oberholzer, H.-R. (2008). Status of earthworm populations after different compaction impacts and varying subsequent soil management practices (pp. 249–256). *Proceedings of the 5th International Soil Conference, ISTRO Czech Branch*.

Le Bissonnais, Y. (2010). Aggregate stability and assessment of soil crustability and erodibility: I. Theory and methodology. *European Journal of Soil Science*, *48*, 39–48. https://doi.org/10.1111/j.1365-2389.1997.tb00183.x

Legland, D., Arganda-Carreras, I., & Andrey, P. (2016). MorphoLibJ: Integrated library and plugins for mathematical morphology with ImageJ. *Bioinformatics*, *32*, 3532–3534.

Lee, K. E. (1985). *Earthworms: Their ecology and relationships with soils and land use*. Academic Press.

Lipiec, J., & Hatano, R. (2003). Quantification of compaction effects on soil physical properties and crop growth. *Geoderma*, *116*, 107–136. https://doi.org/10.1016/S0016-7061(03)00097-1

Martínez, I., Chervet, A., Weisskopf, P., Sturny, W. G., Rek, J., & Keller, T. (2016). Two decades of no-till in the Oberacker long-term field experiment: Part II. Soil porosity and gas transport parameters. *Soil & Tillage Research*, *163*, 130–140.

Michener, C. D. (2007). *The bees of the world* (2nd. ed.). Johns Hopkins.

Muhadiram, N. P. K., Humphreys, M. W., Fychan, R., Davies, J. W., Sanderson, R., & Marley, C. L. (2020). Do agricultural grasses bred for improved root systems provide resilience to machinery-derived soil compaction? *Food and Energy Security*, *9*, e227.

Nawaz, M. F., Bourrie, G., & Trolard, F. (2013). Soil compaction impact and modelling. A review. *Agronomy for Sustainable Development*, *33*, 291–309. https://doi.org/10.1007/s13593-011-0071-8

Nordfjell, T., Öhman, E., Lindroos, O., & Ager, B. (2019). The technical development of forwarders in Sweden between 1962 and 2012 and of sales between 1975 and 2017. *International Journal of Forest Engineering*, *30*, 1–13. https://doi.org/10.1080/14942119.2019.1591074

Olesen, J. E., & Munkholm, L. J. (2007). Subsoil loosening in a crop rotation for organic farming eliminated plough pan with mixed effects on crop yield. *Soil & Tillage Research*, *94*, 376–385.

Or, D., & Ghezzehei, T. A. (2002). Modeling post-tillage soil structural dynamics: A review. *Soil & Tillage Research*, *64*, 41–59.

Or, D., & Lehmann, P. (2019). Surface evaporative capacitance: How soil type and rainfall characteristics affect global-scale surface

evaporation. *Water Resources Research*, *55*. https://doi.org/10.1029/2018WR024050

Or, D., Keller, T., & Schlesinger, W. H. (2021). Natural and managed soil structure: On the fragile scaffolding for soil functioning. *Soil & Tillage Research*, *208*, 104912.

Peng, X., & Horn, R. (2008). Time-dependent, anisotropic pore structure and soil strength in a 10-year period after intensive tractor wheeling under conservation and conventional tillage. *Journal of Plant Nutrition and Soil Science*, *171*, 936–944. https://doi.org/10.1002/jpln.200700084

Perroux, K. M., & White, I. (1988). Designs for disc permeameters. *Soil Science Society of America Journal*, *52*, 1205–1215. https://doi.org/10.2136/sssaj1988.03615995005200050001x

Philips, J. D., & Marion, D. A. (2006). Biomechanical effects of trees on soil and regolith: Beyond treethrow. *Annals of the Association of American Geographers*, *96*, 233–247. https://doi.org/10.1111/j.1467-8306.2006.00476.x

Pinheiro, J., Bates, D., DebRoy, S., Sarkar, D., & R Core Team (2021). *nlme: Linear and Nonlinear Mixed Effects Models*. *R package version 3.1-152*. https://CRAN.R-project.org/package=nlme.

Pulido-Moncada, M., Katuwal, S., Ren, L., Cornelis, W., & Munkholm, L. (2020). Impact of potential bio-subsoilers on pore network of a severely compacted subsoil. *Geoderma*, *363*, 114154. https://doi.org/10.1016/j.geoderma.2019.114154

Qi, J., Vermeer, P. A., & Cheng, G. (2006). A review of the influence of freeze-thaw cycles on soil geotechnical properties. *Permafrost and Periglacial Processes*, *17*, 245–252. https://doi.org/10.1002/ppp.559

Richard, G., Cousin, I., Sillon, J. F., Bruand, A., & Guérif, J. (2001). Effect of compaction on the porosity of a silt soil: Influence on unsaturated hydraulic conductivity. *European Journal of Soil Science*, *52*, 49–58. https://doi.org/10.1046/j.1365-2389.2001.00357.x

Schindelin, J., Arganda-Carreras, I., Frise, E., Kaynig, V., Longair, M., Pietzsch, T., Preibisch, S., Rueden, C., Saalfeld, S., Schmid, B., Tinevez, J.-Y., White, D. J., Hartenstein, V., Eliceiri, K., Tomancak, P., & Cardona, A. (2012). Fiji: An open-source platform for biological-image analysis. *Nature Methods*, *9*, 676–682. https://doi.org/10.1038/nmeth.2019

Schjønning, P., van den Akker, J. J. H., Keller, T., Greve, M. H., Lamandé, M., Simojoki, A., Stettler, M., Arvidsson, J., & Breuning-Madsen, H. (2015). Driver-Pressure-State-Impact-Response (DPSIR) analysis and risk assessment for soil compaction – a European perspective. *Advances in Agronomy*, *133*, 183–237. https://doi.org/10.1016/bs.agron.2015.06.001

Schneider, C. A., Rasband, W. S., & Eliceiri, K. W. (2012). NIH Image to ImageJ: 25 years of image analysis. *Nature Methods*, *9*, 671–675. https://doi.org/10.1038/nmeth.2089

Sonderegger, T., Pfister, S., & Hellweg, S. (2020). Assessing impacts on the natural resource soil in life cycle assessment: Methods for compaction and water erosion. *Environmental Science & Technology*, *54*, 6496–6507.

Suter, D., Rosenberg, E., Frick, R., & Mosimann, E. (2008). Standardmischungen für den Futterbau, Revision 2009–2012. *Agrarforschung Schweiz*, *15*, 1–12.

Tessier, D. (1990). Behavior and microstructure of clay minerals. In M. F. De Boodt, M. H. B. Hayes, & A. Herbillon (Eds.), *Soil colloids and their associations in aggregates*. Plenum Press.

Tuller, M., & Or, D. (2003). Hydraulic functions for swelling soils: Pore scale considerations. *Journal of Hydrology*, *272*, 50–71. https://doi.org/10.1016/S0022-1694(02)00254-8

Vennik, K., Kukk, P., Krebstein, K., Reintam, E., & Keller, T. (2019). Measurements and simulations of rut depth due to single and multiple passes of a military vehicle on different soil types. *Soil & Tillage Research*, *186*, 120–127.

Viklander, P. (1998). Permeability and volume changes in till due to cyclic freeze/thaw. *Canadian Geotechnical Journal*, *35*, 471–477. https://doi.org/10.1139/t98-015

Watanabe, H. (1998). Soil excavation by the deutzia andrenid bee (Andrena prostimias) in a temple garden in Hyogo Prefecture, Japan. *Applied Soil Ecology*, *9*, 283–287. https://doi.org/10.1016/S0929-1393(97)00054-1

Watt, M., Kirkegaard, J. A., & Passioura, J. B. (2006). Rhizosphere biology and crop productivity – a review. *Australian Journal of Soil Research*, *44*, 299–317. https://doi.org/10.1071/SR05142

Weaver, T., & Dale, D. (1978). Trampling effects of hikers, motorcycles and horses in meadows and forests. *Journal of Applied Ecology*, *15*, 451–457. https://doi.org/10.2307/2402604

Weisskopf, P., Reiser, R., Rek, J., & Oberholzer, H.-R. (2010). Effect of different compaction impacts and varying subsequent management practices on soil structure, air regime and microbiological parameters. *Soil & Tillage Research*, *111*, 65–74.

Wilkinson, T., Richards, P. J., & Humphreys, G. S., (2009). Breaking ground: Pedological, geological, and ecological implications of soil bioturbation. *Earth-Science Reviews*, *97*, 257–272. https://doi.org/10.1016/j.earscirev.2009.09.005

Yang, M., Fu, Y., Li, G., Ren, Y., Li, Y., & Ma, G. (2020). Microcharacteristics of soil pores after raindrop action. *Soil Society of America Journal*, *84*, 1693–1704. https://doi.org/10.1002/saj2.20113

SUPPORTING INFORMATION

Additional supporting information may be found online in the Supporting Information section at the end of the article.

How to cite this article: Keller T, Colombi T, Ruiz S, et al. Soil structure recovery following compaction: Short-term evolution of soil physical properties in a loamy soil. *Soil Sci Soc Am J*. 2021;*85:*1002–1020. https://doi.org/10.1002/saj2.20240